Fuel 210 (2017) 507–513

Contents lists available at ScienceDirect

Fuel

journal homepage: www.elsevier.com/locate/fuel

Full Length Article

Total sulfur determination in liquid fuels by ICP-OES after oxidation-extraction desulfurization using magnetic graphene oxide

Mazaher Ahmadi[a,*], Miguel Ángel Aguirre[b], Tayyebeh Madrakian[a], Abbas Afkhami[a], Antonio Canals[b,*]

[a] Faculty of Chemistry, Bu-Ali Sina University, Hamedan, Iran
[b] Department of Analytical Chemistry and Food Science and University Institute of Materials, Faculty of Science, University of Alicante, P.O. Box 99, 03080 Alicante, Spain

ARTICLE INFO

Keywords:
Oxidation-extraction desulfurization
Magnetic graphene oxide
Sulfur determination
Liquid fuel samples
ICP-OES

ABSTRACT

This paper presents a graphene oxide-based magnetic nanocomposite as a catalyst for desulfurization and also as a sorbent for removal of the total sulfur in liquid fuel matrices. The magnetic nanocomposite was prepared by decorating graphene oxide nanosheets with magnetite nanoparticles (MGO). For the desulfurization experiments, an oxidation-extraction procedure was developed using MGO as the catalyst and H_2O_2 as the oxidant. For the sulfur determination experiments, the oxidized-sulfur compounds were sorbed by magnetic solid phase extraction (MSPE) followed by ICP-OES detection. The magnetic nanocomposite showed high efficiency as did both the catalyst of sulfur compounds oxidation and the adsorbent of the oxidized sulfur compounds. Different parameters which could affect the desulfurization and determination were optimized using a multivariate analysis. The results showed that under the optimum conditions removal efficiencies of over 97% were achievable and the limit of detection of 0.15 mg kg^{-1} of sulfur was obtained. Finally, the spiked/recovery assays of commercial fuel samples using MSPE-ICP-OES led to recovery values in the range of 94 ± 5% to 101 ± 3%. The results obtained suggest that a powerful alternative has been developed for the desulfurization and total sulfur determination in commercial fuel samples.

1. Introduction

Daily consumption of liquid fuels such as gasoline, diesel, kerosene, jet fuel, etc. for energy production purposes has led to release various contaminants into the atmosphere. This everyday pollution of the environment should be decreased and managed. Nowadays, there are many strict regulations to control the releasing of different toxic contaminants into the environment. Sulfur oxides and sulfate particulate matters are an important family of toxic compounds subject to health regulations. The presence of sulfur compounds such as sulfides, disulfides, mercaptans and thiophenes in liquid fuels has always been a critical issue for industry and environment [1–6]. In the crude oil refining process, the presence of sulfur compounds leads to deactivation of catalyst materials and also causes pipeline corrosion. On the other hand, the presence of these compounds in fuel leads to the emission of sulfur oxide gasses to the atmosphere which further cause acid rain and also impacts on human health [1]. Furthermore, sulfur oxides in exhaust fumes poison catalysts in catalytic converters and disturb CO and NO_x conversion, and subsequently their emissions to the atmosphere. Therefore, desulfurization is an environmentally and economically critical issue which needs every attention.

Methods available for the desulfurization of liquid fluids can be categorized as hydrodesulfurization (HDS) [7,8], oxidative desulfurization (ODS) and oxidation-extraction desulfurization (OEDS) [9–13], adsorptive desulfurization (ADS) [14–16] and biodesulfurization (BDS) [4,17]. HDS is widely used by industry and involves the reduction of sulfur compounds under relatively harsh conditions (high temperatures and pressures) by hydrogen gas utilizing catalyst materials. In recent years, researchers have attempted to introduce more cost-effective and safer procedures such as ODS, OEDS, ADS and BDS. ADS is based on the extraction of sulfur compounds using a solid sorbent. Although, this method is cheaper and greener, its efficiency is relatively low due to the highly hydrophobic nature of most of the sulfur compounds which are already in a very nonpolar matrix. To improve the extraction efficiency, advanced sorbents such as molecularly imprinted polymers [18] and nanostructured adsorbents have been proposed [19]. Also, protonation or oxidations of sulfur compounds before extraction have been proposed to convert them to more hydrophilic compounds.

* Corresponding authors.
E-mail addresses: m.ahmadi@basu.ac.ir (M. Ahmadi), a.canals@ua.es (A. Canals).

http://dx.doi.org/10.1016/j.fuel.2017.08.104
Received 15 April 2017; Received in revised form 1 August 2017; Accepted 29 August 2017
0016-2361/ © 2017 Elsevier Ltd. All rights reserved.

In oxidative processes (i.e., ODS and OEDS), oxidants such as hydrogen peroxide, peroxy acids, oxygen, etc. are used to oxidize sulfides in liquid fuels to more hydrophilic sulfone compounds. These more hydrophilic compounds can then be removed/extracted from the medium using various extraction techniques such as liquid-liquid or solid-phase extraction. Usually, a catalyst is used to increase the oxidation process efficiency and to decrease the reaction temperature and time appropriately. Furthermore, in order to decrease the total process cost, catalyst materials with dual functionality have been developed (i.e., the catalyst for the oxidation process and the sorbent to extract the oxidation products) [20–24]. In this paper, we report a new nanocomposite with dual functionality not only for OEDS but also for preconcentration of sulfur compounds in liquid fuel matrices prior to inductively coupled plasma optical emission spectrometry (ICP-OES) measurements.

Determination of total sulfur concentration in liquid fuel matrices using ICP-OES has always been a major challenge because direct introduction of organic samples to ICP-OES leads to some serious problems such as the deterioration of the plasma thermal properties [25–27]. Therefore, usually a sample pretreatment/preparation step is used for sulfur determination in liquid fuel matrices such as dilution with an organic solvent, emulsification, decomposition of the sample matrix and extraction (liquid-liquid and solid-phase extraction) [26]. Solid-phase extraction provides some advantages over the other techniques, such as greener extraction (compared to some hazardous solvents used in liquid-liquid extraction), higher enrichment factor (compared to dilution with an organic solvent), time consuming sample preparation (compared to decomposition of the sample matrix by microwave digestion) and generally cheaper and easier procedures. However, one of the drawbacks of this method is the difficulty posed by the solid phase separation from the medium that could be resolved to some extent through the application of magnetic nanoparticle for magnetic solid-phase extraction (MSPE) [28,29].

The adsorbents used in the MSPE technique possess a magnetic phase mainly composed of an iron mineral or iron oxides such as magnetite (Fe_3O_4) or maghemite (γ-Fe_2O_3), and a sorbent, including organic and inorganic polymers and metal oxides. Modified silica (C_{18}, C_8 and phenyl groups), molecularly imprinted polymers and recently, carbon nanotubes, graphene and graphene oxide have been employed [30]. The use of sorbents decorated with magnetic solids synergistically combines the excellent sorbent capacity with easy sorbent handling by means of an external magnetic field.

Herein, magnetic graphene oxide (MGO) has been used as both the catalyst for OEDS and the adsorbent for MSPE extraction of the oxidized sulfur compounds prior to ICP-OES measurements. Hydrogen peroxide and concentrated nitric acid were used as the oxidant and protonating agent, respectively. Different parameters which could affect the MSPE procedure were optimized using a multivariate experimental design. Subsequently, the optimized method was successfully used to remove and determine sulfur compounds in commercial fuel samples (i.e., diesel and gasoline).

2. Experimental

2.1. Reagents and commercial fuel samples

For the synthesis of the magnetic materials, graphene oxide (GO), $FeCl_3{\cdot}6H_2O$ and $(NH_4)_2Fe(SO_4)_2{\cdot}6H_2O$ from Sigma-Aldrich (St. Louis, MO, USA) and ammonium hydroxide solution (32%, w w^{-1}) and ethanol from Scharlau (Barcelona, Spain) were used. Deionized water (resistivity more than 18 MΩ cm) supplied by a water purification system (Milli-Q Biocel A10) from Millipore (Billerica, MA, USA) was used. A Neodymium magnet (Supermagnete, Gottmadingen, Germany) was used for magnetic separation.

Sulfur stock solution in diesel fuel (10,000 mg kg^{-1}) and blank diesel fuel were purchased from SCP Science (Baie D'Urfé, Canada). The working solutions were prepared by diluting the stock solution with kerosene (Sigma-Aldrich). Hydrogen peroxide solution (H_2O_2, 30% w w^{-1}) as the oxidant and concentrated nitric acid solution (HNO_3, 60% w w^{-1}) as the protonating agent were obtained from Sigma-Aldrich. The MSPE procedure was conducted inside 25 mL glass vials (screw top with solid green melamine cap with PTFE liner) from Supelco (Bellefonte, PA, USA).

Commercial diesel and gasoline samples were collected from local gas stations (Alicante, Spain) and were used without undergoing any special pretreatment. The samples were stored in the refrigerator until analyzed. Before performing the analysis, the samples were allowed to reach room temperature. In the case of the determination experiments, the samples were diluted using kerosene to meet the linear calibration range.

2.2. Apparatus and instruments

Size and morphological properties of the synthesized magnetic nanomaterial were investigated using a transmission electron microscope (TEM) from JEOL Co. (JEM-2010, 200 kV, Tokyo, Japan). The crystal structure of the synthesized nanomaterial was determined by an X-ray diffractometer (XRD, D8-Advance, Bruker Daltonics Co., MA, USA) at ambient temperature. SQUID magnetometer MPMS-XL-5 (Quantum Design, CA, USA) was used for magnetic characterization. A 35 kHz universal ultrasonic cleaner water bath (Elma, Singen, Germany) was used for the nanomaterial synthesis and also for the MSPE procedure.

An inductively coupled plasma-optical emission spectrometer (model 720-ES, Agilent Technologies, Melbourne, Victoria, Australia) was used for ICP-OES measurements. Table S1 in the ESI shows the instrumental conditions used and the evaluated emission line. The instrumental conditions were optimized achieving the maximum sulfur intensity using a standard solution containing 20 mg kg^{-1} of sulfur in kerosene.

2.3. Synthesis of magnetic graphene oxide (MGO)

MGO was synthesized based on a co-precipitation method with some modifications [31]. Typically, $FeCl_3{\cdot}6H_2O$ (0.11 g) and $FeCl_2{\cdot}4H_2O$ (0.18 g) were dissolved in 20 mL deionized water (solution A). On the other hand, GO (0.1 g) was dispersed in 200 mL deionized water by sonication for 2 h (solution B). Then, solution A was added to solution B dropwise in 5 min and the mixture was stirred for 30 min at 90 °C. After that, the mixture pH was adjusted at 11 using ammonia solution (32%, w w^{-1}) to form the magnetite nanoparticles. The mixture was stirred continuously for 4 h, then the magnetic nanomaterial (MGO) was separated using an external magnetic field, washed using deionized water and ethanol (3 consecutive times) and dried at 200 °C for 2 h.

For preliminary experiments, magnetite nanoparticles (MNPs) were synthesized using the same procedure except for the addition of the GO nanosheets.

2.4. Optimization of the MSPE procedure

To achieve the highest removal efficiencies and, subsequently, the highest sensitivity in the MSPE procedure, both sorption and desorption steps were optimized separately. All experiments were randomly carried out in order to nullify the effect of extraneous or nuisance factors using a standard solution containing 20 mg kg^{-1} of sulfur in kerosene. Statgraphics Statistical Computer Package “Statgraphics Plus 5.1” (Warrenton, VA, USA) was used to construct experimental design matrices and to evaluate the results.

2.4.1. Optimization of the sorption step (desulfurization)

The desulfurization was optimized by using a multivariate analysis consisting of two steps: (i) a Plackett-Burman design to determine the

significance of the experimental factors affecting the removal efficiency (i.e., HNO_3 and H_2O_2 volumes, MGO amount and sorption time) followed by (ii) a circumscribed central composite design (CCCD) to optimize those factors identified as significant in step (i). Both the screening study using Plackett-Burmann design and the optimization with CCCD involved 12 experiments each. The removal efficiency was used as response and was calculated using the following equation: (Eq. (1))

$$\text{Removal efficiency}(\%) = \left[\frac{(C_0 - C_t)}{C_0}\right] \times 100 \quad (1)$$

where C_0 and C_t represent the initial and final (after removal) total concentrations of the sulfur compounds in mg kg^{-1}, respectively.

2.4.2. Optimization of the desorption step (sulfur determination)

Under optimum conditions for the sorption experiments, the desorption step was optimized. First, different eluents (methanol, ethanol, acetonitrile and a solution of 1.0 M sodium hydroxide) were evaluated to desorb the adsorbed oxidized-sulfur compounds. In the next step, the eluent volume and desorption time were optimized using a CCCD design. The matrix for this CCCD design involved a total of 12 runs. The sulfur emission signal obtained from ICP-OES was used as response.

2.5. Overall MSPE procedure

Fig. 1 shows a schematic description of the MSPE-ICP-OES analysis of sample/calibration standards. For sulfur sorption by MSPE procedure, 50 µL HNO_3 (60% w w^{-1}) was added to 20 mL of sample/calibration standard. Then, 20 mg MGO and 500 µL H_2O_2 (30% w w^{-1}) were added consecutively. The mixture was sonicated at room temperature for 33 min. Then, the magnetic nanocomposite which contains the oxidized-sulfur compounds was separated using a hand-held magnet and the concentration of sulfur compounds in the supernatant was measured using the ICP-OES in order to obtain the recovery efficiency values.

For sulfur determination by MSPE procedure, the magnetic nanocomposite which contains the oxidized-sulfur compounds was washed twice with pure kerosene (5 mL and 5 min sonication) and was eluted with methanol (200 µL and 6.6 min sonication) at room temperature. After that, the magnetic nanocomposite and the eluate were magnetically separated. Finally, the eluate was introduced to the ICP-OES instrument.

Table 1
Figures of merit of the proposed MSPE-ICP-OES method for the determination of total sulfur under the optimized conditions.

Parameter	MSPE-ICP-OES	ICP-OES
Linear working range[a] (mg kg^{-1})	0.5–5.0	5.0–20.0
Correlation linear coefficient[a]	0.9993	0.9983
LOD (mg kg^{-1})	0.15	1.4
LOQ (mg kg^{-1})	0.5	4.6
Sensitivity (cps mg μg^{-1})	3373 ± 61	176 ± 7
Relative sensitivity[b]	19.2 ± 0.5	–
Relative LOD[c]	9.3	–

[a] Number of calibration points = 6.
[b] Sensitivity of the MSPE-ICP-OES to sensitivity of ICP-OES.
[c] LOD of ICP-OES to LOD of the MSPE-ICP-OES.

2.6. Analytical figures of merit

In order to assess the analytical capability of the MSPE-ICP-OES procedure versus ICP-OES for the sulfur determination in kerosene matrix, analytical figures of merit (i.e., linear working range, sensitivity, LOD and LOQ) of both analytical procedures were evaluated and compared (Fig. 1 and Table 1). To this end, calibration standards were analyzed by both methods in order to obtain the corresponding calibration graphs: (i) without a previous MSPE procedure (direct ICP-OES analysis of the standards); and (ii) after sorption of the analytes by MSPE under optimum conditions. In the former method, calibration was performed by directly analyzing six calibration standards with increasing concentrations of sulfur up to 20 mg kg^{-1}. In the latter, sulfur was extracted from the same number of calibration standard solutions but with increasing concentrations of sulfur up to 5 mg kg^{-1}. The relative narrow working range is mainly because of the MGO amount available. Wider working range can be obtained by using larger MGO quantity.

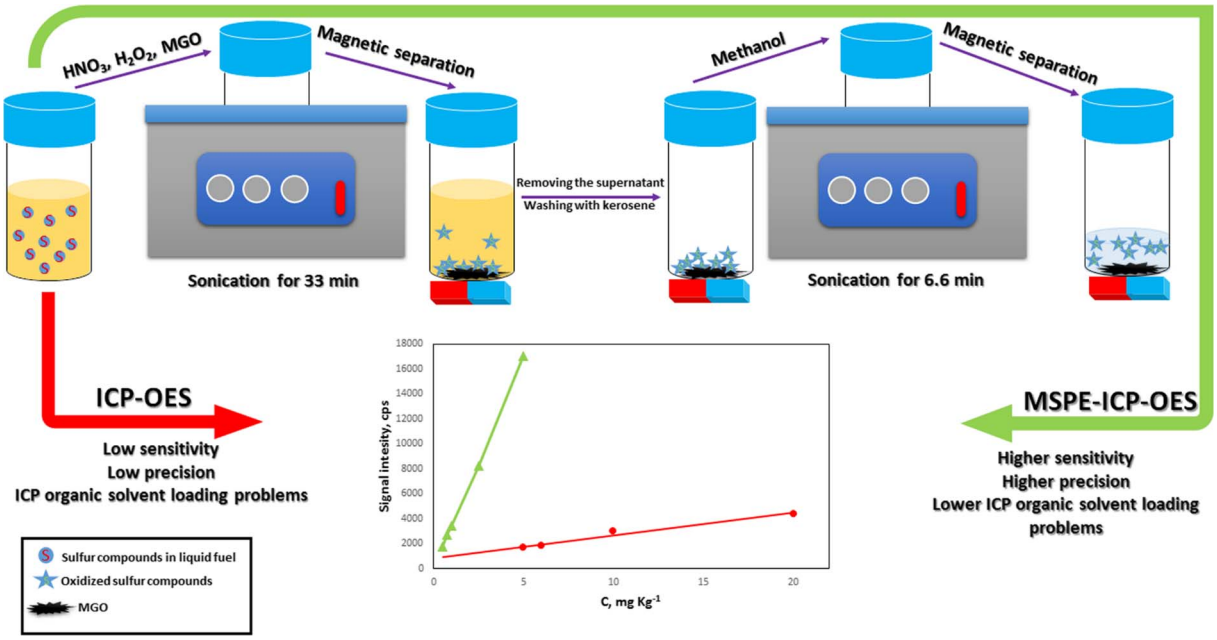

Fig. 1. Schematic description of the proposed MSPE-ICP-OES method.

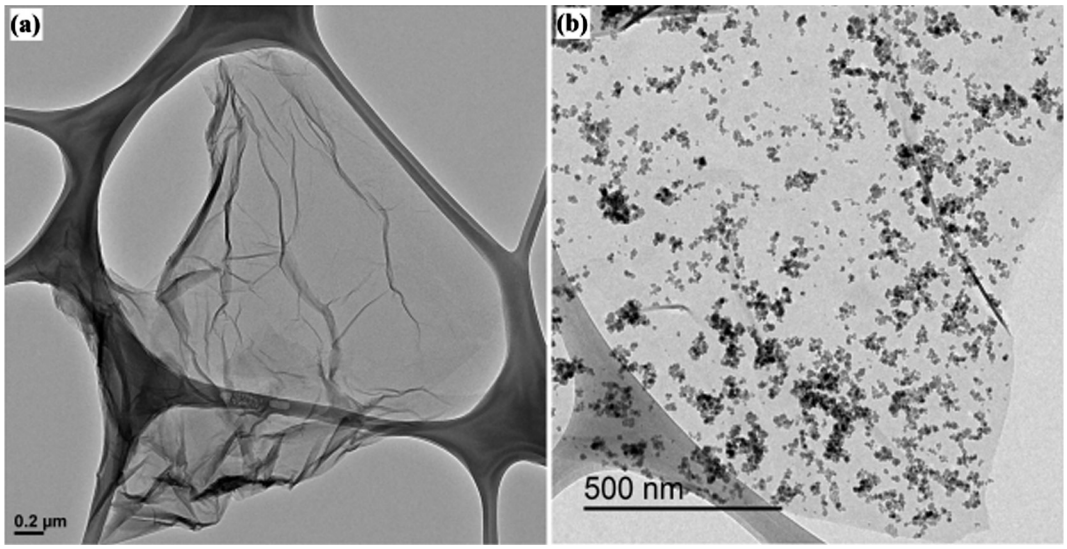

Fig. 2. TEM images of (a) the bare GO and (b) the MGO nanomaterial.

3. Results and discussion

3.1. Characterization of the synthesized magnetic nanomaterial

Fig. 2 shows the nanomaterials TEM images, wherein TEM image of bare graphene oxide nanosheets is presented as Fig. 2a. Fig. 2b shows that the nanosheets are successfully modified by MNPs. As noted, the nanosheets are almost uniformly modified by the magnetic nanoparticles with an average size of 14 ± 3 nm.

Fig. 3 shows the magnetization hysteresis loop of MGO. The magnetization hysteresis loop of MGO was S-like curve indicating that the composite was superparamagnetic material. The specific magnetization saturation (Ms) was 38.5 emu g^{-1}.

The XRD pattern of the synthesized magnetic nanomaterial is presented in Fig. 4. The XRD pattern of the synthesized MGO (Fig. 4b) shows diffraction peaks that are indexed to (2 2 0), (3 1 1), (4 0 0), (4 2 2), (5 1 1) and (4 4 0) reflection characteristics of cubic spinel phase of Fe_3O_4 (JCPDS powder diffraction data file No. 79-0418), revealing that the resultant MGO is successfully loaded by mostly magnetite nanoparticles [32].

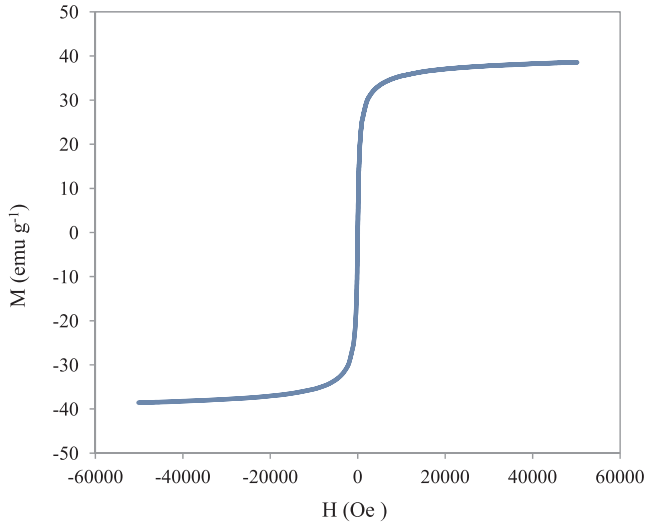

Fig. 3. The magnetization hysteresis loop of MGO.

3.2. Preliminary experiments

In order to evaluate the mechanism and the roles of experimental variables (i.e., HNO_3, H_2O_2 and MGO on the sulfur compounds removal), preliminary experiments were performed in the absence of each component (Fig. 5a) and also using different nanoparticles with presence in the final nanocomposite composition (i.e., bare GO and MNPs) (Fig. 5b).

The results (Fig. 5a) showed that combination of HNO_3, H_2O_2 and MGO led to the highest removal efficiencies. Moreover, HNO_3 proved to have the most critical role (i.e., the lowest removal efficiency was obtained in the absence of the acid) suggesting that if the sulfur compound is not protonated, it cannot be involved in the aqueous phase oxidation reaction because of the high hydrophobicity. The experiments in the absence of MGO showed that the presence of the nanocomposite was necessary in order to reach high removal efficiencies. MGO may act either as the catalyst of the oxidation reaction or the adsorbent to remove the oxidation product from the medium or both. To clarify the nanocomposite role, the two main components of MGO (MNPs and GO) were utilized in separate experiments for removal of sulfur compound from kerosene (Fig. 5b). The results showed that the presence of the two main components as a nanocomposite in MGO produces a synergistic effect. As noted in Fig. 5b, MNPs led to higher removal efficiencies than GO. In fact, MNPs can be partially dissolved in the presence of the acid producing free ferric and ferrous ions as observed practically leading to catalysis as in the oxidation reaction based on Fenton's reagent concept [33]. This effect can be followed by partial adsorption of the oxidation products by MNPs and liquid-liquid extraction leading to the obtained removal efficiencies. On the other hand, GO can act more efficiently as an adsorbent because of its outstanding features such as high surface area, the presence of high degree of aromatic rings available for π-π interactions and also carboxylic acid and hydroxyl groups available for hydrophilic interactions [34–36]. Therefore, the presence of these two components in MGO composition has led to the highest removal efficiencies.

3.3. Optimization of sorption step (desulfurization)

After this preliminary investigation, various important parameters which could affect the removal efficiencies including HNO_3 and H_2O_2 volumes, MGO amount and sorption time were firstly screened using a Plackett-Burman design (Table S2 in the ESI). The results from Fig. S1 in the ESI showed that all the parameters investigated had positive

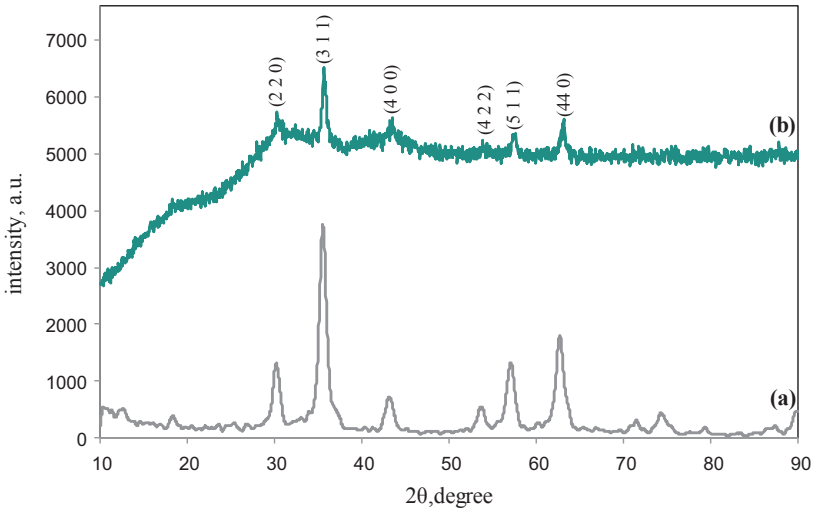

Fig. 4. The XRD patterns of (a) magnetite nanoparticles and (b) the MGO nanomaterial.

effects except H_2O_2 volume. However, only the effects of the MGO amount and sorption time were statistically significant (at 95% confidence interval). Therefore, the effects of the MGO amount and sorption time were optimized using a CCCD design (Table S3 in the ESI) at fixed values for the acid and the oxidant (i.e., the high level for the acid, 50 μL, the low level for the oxidant, 500 μL). The results of the 12 experiments of the CCCD design are shown in Fig. S2 in the ESI. As expected, both experimental factors revealed positive effects on the sorption step. In the case of sorption time, the removal efficiency increases by increasing sonication time up to 33 min and then tends to be stable suggesting that a semi-equilibrium condition has been reached. The optimum conditions for the removal experiments obtained using the multivariate method was: 20 mg of MGO and 33 min of sorption time. In sum, the optimized values which were further considered for the sorption step of the MSPE procedure are: MGO amount, 20 mg; sorption time, 33 min; HNO_3 and H_2O_2 volumes, 50 and 500 μL, respectively.

3.3.1. Optimization of desorption step (sulfur determination)

Under the optimized condition for the sorption step, desorption experiments were conducted at room temperature. First, different eluents (methanol, ethanol, acetonitrile and 1.0 mol L^{-1} of sodium hydroxide solution) were evaluated to desorb the adsorbed oxidized-sulfur compounds and the results (Fig. S3 in the ESI) showed that, among the investigated eluents, methanol is the best back-extractor solvent. In the next step, methanol volume and desorption time were optimized using a CCCD design (Table S4 in the ESI). As it can be seen from Fig. S4 in the ESI, the desorption time shows a positive effect at low desorption times and a negative effect at high desorption times upon desorption resulting in a maximum sulfur recovery at around 6.6 min. Therefore, prolonged desorption times might conceivably lead to re-adsorption of sulfur compounds [37]. On the other hand, methanol volume also shows a similar effect resulting in a maximum amount of sulfur eluted at approximately 200 μL. The negative effect at high methanol volumes can be attributed to the dilution effect.

3.4. Analytical figures of merit

Under optimum conditions for the MSPE procedure (i.e., MGO amount, 20 mg; sorption time, 33 min; HNO_3 volume: 50 μL; H_2O_2 volume: 500 μL, eluent solvent: methanol; elution volume: 200 μL and desorption time: 6.6 min), a linear calibration graph was constructed for six different initial concentrations of sulfur compounds in kerosene ranging from 0.5 to 5.0 mg kg^{-1} (Table 1). Wider working range can be obtained using a larger MGO quantity.

Table 1 shows the analytical figures of merit of both ICP-OES and MSPE-ICP-OES total sulfur analysis. The sensitivity values were obtained from the slope of the calibration curves (see Section 2.6). The limit of detection (LOD) calculation was based on three times the standard deviation of blank standards (kerosene for ICP-OES and methanol for MSPE-ICP-OES), whereas the limit of quantification (LOQ) was based on ten times the standard deviation of the blank standards. As noted, the use of the MSPE procedure has led to lower LOD and LOQ in comparison to direct introduction of the samples to the detection instrument. Also, the measurement sensitivity has been considerably increased (~19-fold) by applying the MSPE procedure on the samples before their introduction to the ICP-OES spectrometer. Furthermore, a comparison of the figures of merit of the proposed method with

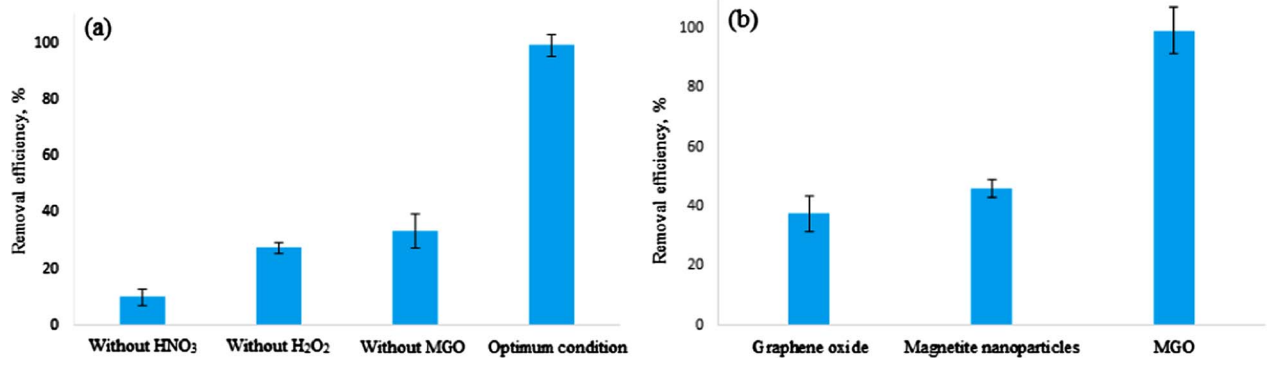

Fig. 5. Effect of the acid, oxidant and adsorbent addition (a) and effect of different nanoparticles (b) on sulfur compounds removal efficiency (conditions: 20 mL of 20 mg kg^{-1} of sulfur in kerosene, 50 μL HNO_3 (60% w w^{-1}), 500 μL H_2O_2 (30% w w^{-1}), 20 mg MGO or GO or MNPs, 33 min sonication at room temperature, n = 3).

Table 2
Comparison of the previously ICP-OES based methods for total sulfur determination in liquid fuel matrices.

Sample preparation	Matrix	Linear range (mg kg^{-1})	LOD (mg kg^{-1})	LOQ (mg kg^{-1})	Ref.
Dilution in xylene	Crude oil and petroleum products	–	100	–	[39]
Dilution in ethanol or n-propanol	Biodiesel	0.6–30	0.4	1.3	[40]
Emulsion preparation using ethoxy nonylphenol, xylene and water	Crude oil	270–825	0.6	–	[41]
Emulsion preparation using nitric acid, Triton X-100 and water	Kerosene, diesel and gasoline	20–200	0.72	2.4	[38]
Microwave-induced combustion using glass wool as a flame retardant	Diesel	–	2	6.9	[42]
MSPE-ICP-OES	Kerosene, diesel and gasoline	0.5–5.0	0.15	0.5	This work

Table 3
Analysis of the real fuel samples using the proposed MSPE-ICP-OES method and ICP-OES.

Sample	Removal efficiency (%)	Found by the proposed method[a] (mg kg^{-1})	Found by standard addition-ICP-OES[b] (mg kg^{-1})	R[c] (%)
Diesel				
Without spiking	97.6	17.00 ± 0.04	16 ± 3	106 ± 21
Spiked at 1 mg kg^{-1}	99.0	17.94 ± 0.03	–	94 ± 5
Spiked at 3 mg kg^{-1}	98.6	19.88 ± 0.03	–	96 ± 5
Gasoline				
Without spiking	98.4	21.70 ± 0.03	22 ± 4	99 ± 17
Spiked at 1 mg kg^{-1}	97.2	22.71 ± 0.02	–	101 ± 3
Spiked at 3 mg kg^{-1}	98.6	24.691 ± 0.015	–	100 ± 3

[a] Uncertainty was estimated as the standard deviation of the interpolated concentration.
[b] Uncertainty was estimated as the standard deviation of the extrapolated concentration.
[c] R: Recovery ± combined standard uncertainty. The combined standard uncertainty was calculated assuming that spiked.

Table 4
Comparison of some previously developed oxidative processes for desulfurization of liquid fuels.

Reagent	Matrix	Time (min)	Temperature (°C)	Removal efficiency (%)	Ref.
H_2O_2 + WO_3/graphitic carbon nitride + ionic liquid	Simulated fuel oil (n-octane)	180	60	91.2	[43]
tert-butyl hydroperoxide + HPWA-SBA-15	Simulated fuel oil (*iso*-octane)	120	70	97.34	[44]
H_2O_2 + formic acid	Simulated fuel oil (toluene: hexane, 40:60)	120	50	92	[45]
H_2O_2 + $ZnCl_2$ + ionic liquid	Diesel	120	50	98.5	[46]
H_2O_2 + Mo/γ-Al_2O_3	Diesel	60	60	97	[47]
H_2O_2 + activated carbon + formic acid	Diesel	60	60	82.3	[48]
H_2O_2 + cerium oxide-loaded molecular sieve 5 A + formic Acid	Simulated fuel oil (n-heptane)	60	50	82.3	[49]
K_2FeO_4 + manganese (III) acetate + acetic acid	Simulated fuel oil (petroleum ether)	45	17 and 25	96.7	[50]
H_2O_2 + Na_2WO_4 + acetic acid	Diesel	30	70	97	[51]
H_2O_2 + ion exchange resin immobilized 12-tungstophosphoric acid	Diesel	8	60	93.5	[52]
H_2O_2 + MGO + nitric acid	Diesel and gasoline	33	21	> 97	This work

previously reported ICP-OES based methods (Table 2) shows that a powerful alternative method has been developed. In sum, as expected, application of the MSPE procedure can enhance sensitivity of the method in comparison to direct introduction of the samples into the detection instrument. But this is not the only advantage of the proposed method. In this work, the sulfur compounds have been extracted from a very problematic solvent (i.e., kerosene) to a more plasma-compatible solvent (i.e., methanol) leading to suppressed deterioration of the thermal plasma properties and extinction problems [25,26,38]. Furthermore, the clean samples (i.e., samples containing low sulfur concentration) can be used after the desulfurization process.

3.5. Analysis of commercial fuel samples

In order to assess the applicability of the MSPE-ICP-OES, a recovery study was evaluated in commercial fuel samples (i.e., diesel and gasoline samples). The added concentrations were 1 and 3 mg kg^{-1} of sulfur. The initial total sulfur concentrations found by the proposed method using external calibration method were 17.00 ± 0.04 and 21.70 ± 0.03 mg kg^{-1} for diesel and gasoline, respectively (Table 3). The corresponding results obtained using the proposed method were in a good agreement with the ICP-OES analysis using standard addition calibration. Recovery values for initial total sulfur concentration show high accuracy of the proposed method (i.e., 106 ± 21 for diesel sample and 99 ± 17 for gasoline sample). In addition, recovery values achieved in all spiked fuel samples evaluated comprise from 94 ± 5 to 101 ± 3. The results of Table 3 show that the method provides a highly accurate determination of total sulfur concentration and high sulfur-removal efficiency in the investigated samples. Also, the method showed high removal efficiency values of sulfur compounds from the commercial fuel samples (removal efficiencies of over 97% for both diesel and gasoline samples). Considering the optimum conditions and the obtained removal efficiencies, the developed method can be considered an excellent alternative for oxidative desulfurization process. As noted in Table 4, in comparison to some previously developed oxidative desulfurization processes, the proposed method provides high removal efficiencies at reasonable reaction time and temperature suggesting the feasibility and cost-effectiveness of the method.

4. Conclusions

The results of this study showed that the application of MGO as both

the adsorbent and the catalyst of the oxidation process in OEDS could provide a powerful method not only for desulfurization purposes but also for determination of total sulfur concentration in liquid fuel matrices by MSPE-ICP-OES. The outstanding features of the proposed method for desulfurization are: (i) MGO acts as both the adsorbent and the catalyst; (ii) the reaction is performed at room temperature unlike other previously developed methods which used relatively high temperatures; (iii) the reaction time is reasonable; (iv) the used chemicals are commercially available and the catalyst synthesis procedure is simple; and (v) the catalyst is magnetically removable and there is no need for high-speed centrifugation or filtration. Furthermore, the proposed method acts as a MSPE step for preconcentration of the oxidized sulfur compounds and facilitates the ICP-OES measurements by improving the sensitivity and suppressing the deterioration of the thermal plasma properties and extinction problems.

Acknowledgement

The authors would like to thank the Spanish Ministry of Science and Innovation (project n. CTQ2011-23968), Generalitat Valenciana (Spain) (project n. PROMETEO/2013/038) for the financial support, and Agilent Technologies Inc. for the loan of the ICP-OES spectrometers. M. Ahmadi would like to thank the Iranian Ministry of Science, Research and Technology for the travel grant.

Appendix A. Supplementary data

Supplementary data associated with this article can be found, in the online version, at http://dx.doi.org/10.1016/j.fuel.2017.08.104.

References

[1] Chandra Srivastava V. RSC Adv 2012;2:759–83.
[2] Feng M. Rec Pat Chem Eng 2010;3:30–7.
[3] Bhutto AW, Abro R, Gao S, Abbas T, Chen X, Yu G. J Taiwan Inst Chem Eng 2016;62:84–97.
[4] Mohebali G, Ball AS. Int Biodeterior Biodegradation 2016;110:163–80.
[5] Abro R, Abdeltawab AA, Al-Deyab SS, Yu G, Qazi AB, Gao S, et al. RSC Adv 2014;4:35302–17.
[6] Yu M, Zhang N, Fan L, Zhang C, He X, Zheng M, et al. Rev Chem Eng 2015;31:27–43.
[7] Fang X, Guo R, Yang C. Chin J Catal 2013;34:130–9.
[8] Ali SA. Appl Petrochem Res 2014;4:409–15.
[9] Ismagilov Z, Yashnik S, Kerzhentsev M, Parmon V, Bourane A, Al-Shahrani FM, et al. Catal Rev 2011;53:199–255.
[10] Jiang Z, LÜ H, Zhang Y. Chin J Catal 2011;32:707–15.
[11] Danlin Z, Yi H, Kemiao W, Guanghui W. Petrol Process Petrochem 2012;43:98–102.
[12] Xiao J, Wu L, Wu Y, Liu B, Dai L, Li Z, et al. Appl Energy 2014;113:78–85.
[13] Choi AES, Roces S, Dugos N, Wan M-W. Fuel 2016;180:127–36.
[14] Samokhvalov A, Tatarchuk BJ. Catal Rev 2010;52:381–410.
[15] Zhang J, Liu Y, An G, Chai Y, Fu Q, Liu C. Progr Chem 2008;20:1834–45.
[16] Yu L, Zhang Y, Chen R, Zhang D, Wei X, Chen F, et al. Xu M. Talanta 2015;131:475–9.
[17] Boniek D, Figueiredo D, dos Santos AFB, de Resende Stoianoff MA. Clean Technol Environ Policy 2015;17:29–37.
[18] Yang YZ, Liu XG, Xu BS. New Carbon Mater 2014;29:1–14.
[19] Saleh TA. Applying nanotechnology to the desulfurization process in petroleum engineering. IGI Global; 2015.
[20] Ren X, Miao G, Xiao Z, Ye F, Li Z, Wang H, et al. Fuel 2016;174:118–25.
[21] Bazyari A, Khodadadi AA, Haghighat Mamaghani A, Beheshtian J, Thompson LT, Mortazavi Y. Appl Catal B 2016;180:65–77.
[22] Xiong J, Zhu W, Li H, Xu Y, Jiang W, Xun S, et al. AIChE J 2013;59:4696–704.
[23] Xiao J, Wang X, Fujii M, Yang Q, Song C. AIChE J 2013;59:1441–5.
[24] Ye F, Miao G, Wu L, Wu Y, Li Z, Song C, et al. Chem Eng Sci 2017;168:225–34.
[25] Nie XD, Xie HL. Spectrosc Spectr Anal 2016;36:1464–7.
[26] Sánchez R, Todolí JL, Lienemann C-P, Mermet J-M. Spectrochim Acta, Part B 2013;88:104–26.
[27] Aguirre MA, Kovachev N, Hidalgo M, Canals A. J Anal At Spectrom 2012;27:2102–10.
[28] Šafaříková M, Šafařík I. J Magnet Magnet Mater 1999;194:108–12.
[29] Aguilar-Arteaga K, Rodriguez JA, Barrado E. Anal Chim Acta 2010;674:157–65.
[30] Costa dos Reis LV L, Canals A. Anal Bioanal Chem 2017.
[31] Madrakian T, Afkhami A, Ahmadi M. Spectrochim Acta Part A, Mol Biomol Spectrosc 2012;99:102–9.
[32] Madrakian T, Ahmadi M, Afkhami A, Soleimani M. Analyst 2013;138:4542–9.
[33] Dai Y, Qi Y, Zhao D, Zhang H. Fuel Process Technol 2008;89:927–32.
[34] Kyzas GZ, Deliyanni EA, Matis KA. J Chem Technol Biotechnol 2014;89:196–205.
[35] Ibrahim WAW, Nodeh HR, Sanagi MM. Crit Rev Anal Chem 2016;46:267–83.
[36] Andrade-Eiroa A, Canle M, Leroy-Cancellieri V, Cerdà V. TrAC – Trends Anal Chem 2016;80:641–54.
[37] Hii TM, Basheer C, Lee HK. J Chromatogr A 2009;1216:7520–6.
[38] Santelli RE, Oliveira EP, De Carvalho MdFB, Bezerra MA, Freire AS. Spectrochim Acta, Part B 2008;63:800–4.
[39] Fabec JL, Ruschak ML. Anal Chem 1985;57:1853–63.
[40] Chaves ES, de Loos-Vollebregt MTC, Curtius AJ, Vanhaecke F. Spectrochim Acta, Part B 2011;66:733–9.
[41] Murillo M, Chirinos J. J Anal At Spectrom 1994;9:237–40.
[42] Cruz SM, Tirk P, Dalla Nora FM, Schmidt L, Wiltsche H, Bizzi CA, et al. Fuel 2015;160:108–13.
[43] Zhao R, Li X, Su J, Gao X. Appl Surf Sci 2017;392:810–6.
[44] Yang L, Li J, Yuan X, Shen J, Qi Y. J Mol Catal A: Chem 2007;262:114–8.
[45] Ali MF, Al-Malki A, El-Ali B, Martinie G, Siddiqui MN. Fuel 2006;85:1354–63.
[46] Yang H, Jiang B, Sun Y, Hao L, Huang Z, Zhang L. Chem Eng J 2016;306:131–8.
[47] García-Gutiérrez JL, Fuentes GA, Hernández-Terán ME, García P, Murrieta-Guevara F, Jiménez-Cruz F. Appl Catal A 2008;334:366–73.
[48] Yu G, Lu S, Chen H, Zhu Z. Carbon 2005;43:2285–94.
[49] Chen L, Guo S, Zhao D. Chin J Chem Eng 2007;15:520–3.
[50] Liu S, Wang B, Cui B, Sun L. Fuel 2008;87:422–8.
[51] Al-Shahrani F, Xiao T, Llewellyn SA, Barri S, Jiang Z, Shi H, et al. Appl Catal B 2007;73:311–6.
[52] Liu R, Zhang Y, Ding J, Wang R, Yu M. Sep Purif Technol 2017;174:84–8.